

Electroluminescent Characteristics of DBPPV–ZnO Nanocomposite Polymer Light Emitting Devices

M. V. Madhava Rao · Yan Kuin Su ·
Tsung Syun Huang · Chen-Han Yeh ·
Ming-Lung Tu

Received: 5 August 2008 / Accepted: 27 January 2009 / Published online: 18 February 2009
© to the authors 2009

Abstract We have demonstrated that fabrication and characterization of nanocomposite polymer light emitting devices with metal Zinc Oxide (ZnO) nanoparticles and 2,3-dibutoxy-1,4-poly(phenylenevinylene) (DBPPV). The current and luminance characteristics of devices with ZnO nanoparticles are much better than those of device with pure DBPPV. Optimized maximum luminance efficiencies of DBPPV–ZnO (3:1 wt%) before annealing (1.78 cd/A) and after annealing (2.45 cd/A) having a brightness 643 and 776 cd/m² at a current density of 36.16 and 31.67 mA/cm² are observed, respectively. Current density–voltage and brightness–voltage characteristics indicate that addition of ZnO nanoparticles can facilitate electrical injection and charge transport. The thermal annealing is thought to result in the formation of an interfacial layer between emissive polymer film and cathode.

Keywords Polymer light emitting devices · Electroluminescent · ZnO nanoparticle · Surface morphology · Thermal annealing

Introduction

Polymer light emitting devices (PLEDs) have attracted much attention in recent years, due to their potential applicability to flat, large area displays [1–3]. Major important technological issues related to commercial

applications are the quantum efficiency, device stability and easy fabrication. Among the conjugated polymers, polyphenylenevinylene (PPV)-based light emitting diodes are limited by their low quantum efficiency as well as poor stability. In spite of these critical drawbacks, the PLED is still receiving considerable attention due to its several merits; they are easy to fabricate with low cost, low operating voltage, flexibility, etc. Therefore, a lot of researches have focused on solving the problem of low efficiency and the poor stability [4–6]. One of the major reasons for the low quantum efficiency of single layer PLEDs is that the electron injection is more difficult than hole injection in most PLEDs due to high energy barrier to electron injection and low electron mobility in most conjugated polymers. Therefore, one of the most important challenges in the field of PLEDs is to improve the balanced charge carrier injection that is essential for high efficiency. Charge carrier mobility plays an important role in determining electroluminescence device performance, which is closely related to the balance between injection and transport of holes and electrons [1–3]. To enhance luminance efficiency, high charge carrier mobility is required. One way to overcome the electron injection and transport limitations is to combine polymers with inorganic semiconductors, which have low energy barrier to electron injection and high electron mobility. However, there have been many reports on how to balance the combination of hole and electron injected from the electron injection from anode and cathode [7–11]. Semiconducting nanoparticles into polymer matrices is an area of current interest in organic nanoelectronics. Such an integration of organic and inorganic materials of the nanometer scale into hybrid optoelectronic structures allows designing devices that combine the diversity and processibility of organic materials with high electronic and optical performance of inorganic nanocrystals [12–17].

M. V. Madhava Rao (✉) · Y. K. Su · T. S. Huang ·
C.-H. Yeh · M.-L. Tu
Institute of Microelectronics, Department of Electrical
Engineering, Advanced Optoelectronic Technology Center,
National Cheng Kung University, Tainan 701, Taiwan, ROC
e-mail: madhavamora@yahoo.com

In this study, nanoparticles composite materials consisting of conjugated polymers and metal oxides are the focus of interest due to their physical, electronic and optical properties. An n-type semiconductor material ZnO possesses a direct wide band gap (3.2 eV), a large exciton binding energy (60 meV) with strong piezoelectric and pyroelectric properties. It is one of the most promising candidates for the fabrication of short wavelength optoelectronic devices [18–20]. To our best knowledge, this could be the first report of PLEDs, which consists of DBPPV and the inorganic semiconductor metal oxide (ZnO).

Experimental Procedure

2,3-dibutoxy-1,4-poly(phenylenevinylene) (DBPPV) was purchased from Eternal Chemical and used without further purification. LEDs with an ITO/PEDOT:PSS/DBPPV–ZnO/Ca/Al structure were fabricated using the following procedures. Patterned ITO-Coated glass substrates were cleaned with detergent, distilled water, acetone and 2-propanol and subsequently in ultrasonic bath. The substrates were dried in an oven at 100 °C, before treatment with UV–Ozone. After treatment with UV–Ozone for 25 min, a 40-nm layer of PEDOT:PSS was spin-coated onto the substrates, followed by drying on a hotplate at 150 °C for 30 min. Commercially available ZnO nanorods of diameter (30–50 nm) and length (1 μm) were purchased from Sigma-Aldrich Corporation. The PLEDs of the DBPPV–ZnO composite single layer were fabricated as follows: polymer–nanoparticle composite films were made either by first dispersing the nanoparticles in the same solvent that the DBPPV is dissolved in, namely toluene, and then adding this mixture to the DBPPV–toluene solution or by adding the nanoparticles directly to the DBPPV–toluene solution. The weight ratios of DBPPV versus ZnO were changed from 4:1 to 2:1 for DBPPV–ZnO (4:1 by wt%) [DB4–ZnO], DBPPV–ZnO (3:1 by wt%) [DB3–ZnO] and DBPPV–ZnO (2:1 by wt%) [DB2–ZnO]. The former technique resulted in better dispersion of the nanoparticles in the final film. Nanocomposite single layers of DBPPV–ZnO were spin-coated from toluene solutions with a speed of 3,000 rpm for 1 min on top of the PEDOT:PSS. This was followed by baking on a hotplate at 60 °C for 30 min inside the glow box. Then, the Ca (60 nm) and the Al (120 nm) electrodes were thermally evaporated in a vacuum of about 2×10^{-6} Torr. For comparison, ITO/PEDOT:PSS/DBPPV/Ca/Al device with thickness around 80–90 nm DBPPV was fabricated according to the similar procedure. The annealing steps were undertaken on a hot plate inside the glow box at 120 °C for 30 min. For the measurement of device

characteristics, current density–voltage (I – V) and brightness–voltage (B – V) changes were measured using a power supply (Keithley 2400) and a fluorescence spectrophotometer (Ocean optics usb 2000), and the luminance was further corrected by SpectaScan PR650 spectrophotometer.

Atomic Force Microscopy (AFM, DI dimension 3100) was used to monitor the surface morphology of films. The surface topography images of the films were coated on the ITO/PEDOT:PSS surfaces. The AFM images are measured over an area of $3 \times 3 \mu\text{m}^2$. AFM is the surface described by cantilever during scan, due to the tip–sample interaction. This leads to the equipforce surface image limited by a convolutive interaction, because the roughness values are influenced by tip, scan size. The main parameters for profile evaluation are defined as [21].

Average roughness (R_a)—the arithmetic average of a deviation y , from the center line is:

$$R_a = \frac{1}{L} \int_0^L |y| dx.$$

Root-mean-square roughness (R_{rms}) is the root-mean-square deviation from center line:

$$R_{\text{rms}} = \left(\frac{1}{L} \int_0^L y^2 dx \right)^{1/2}.$$

For each sample, the rms roughness and average roughness as defined in [21] were evaluated.

The active area of the electroluminescence (EL) devices by overlapped of the ITO and the cathode electrodes was 6 mm^2 .

Results and Discussion

Figure 1a and b shows that the current density versus voltage (I – V) and brightness versus voltage (B – V) characteristics of pure DBPPV, DB2–ZnO, DB3–ZnO and DB4–ZnO devices in a standardized device configuration of ITO/PEDOT:PSS/DBPPV–ZnO/Ca/Al. The device with ZnO-doped DBPPV shows significantly better performance characteristics than those of pure DBPPV, with a considerable current increase in low voltage and higher current density at the same voltage. In addition, the DB3–ZnO device possesses a lower turn voltage (V_{on}) (3.10) and higher brightness at the same voltage (1,639 cd/m^2 at 5 V) than those obtained that pure DBPPV (V_{on}) (3.76, 745 cd/m^2 at 5 V). The maximum brightness of the DB4–ZnO reaches 9,490 cd/m^2 (7.51 V), which is much higher than that of DBPPV (5,004 cd/m^2 at 7.41 V). Figure 2a shows the luminance efficiency versus current density characteristics for the devices. Optimized luminance efficiency could reach 1.78 Cd/A with DB3–ZnO at a current density of 36.16 mA/cm^2 and a brightness of 643 cd/m^2 .

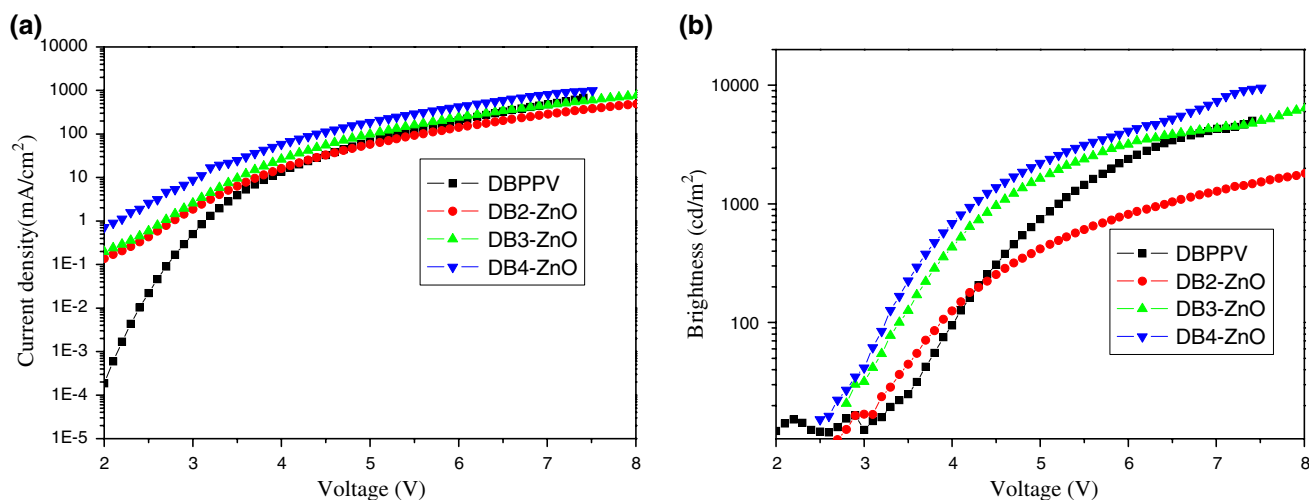


Fig. 1 **a** Current density–voltage (I – V) and **b** brightness–voltage (B – V) characteristics of of DBPPV, DB2–ZnO, DB3–ZnO and DB4–ZnO devices

A maximum brightness of 4,317 cd/m² at 7 V was measured. The electrical characteristics of nanocomposite based PLEDs are summarized in Table 1. The current turn-on voltage (V_{T-on}) of ca.3.76 (pure DBPPV) and 3.10 (DB3–ZnO), at the current of 0.5 mA, which is the majority carrier injection voltage. The DB3–ZnO device had a low turn-on voltage (3.255 V) at a brightness of 100 cd/m², which is 0.76 V lower than that of the pure DBPPV. Lowering turn-on voltage of PLED devices leads to improved current efficiency. Carter and Ligman also observed that radiance–voltage and current–voltage curves for 1:1 TiO₂ (anatase)/MEHPPV, 1:1 TiO₂ (rutile)/MEHPPV, 1:1 SiO₂/MEHPPV and for MEHPPV film without nanoparticles. It is evident that a lower driving voltage can

be achieved using TiO₂ or SiO₂ nanoparticles, than that achieved with pure the MEHPPV film [22, 23].

The increased current by the addition of ZnO nanoparticles may be attributed in part to the ease of charge transport. The ZnO nanoparticles dispersed in the polymer may reduce the barrier for hopping, which may cause increase in carrier density. The enhancement of charge injection and transport may play roles together for the enhancement of EL property by the addition of ZnO nanoparticles. The highest occupied molecular orbital (HOMO) (5.43 eV) and the lowest unoccupied molecular orbital (LUMO) (2.75 eV) levels of DBPPV and the valence (7.6 eV) and conduction (4.4 eV) bands of ZnO clearly indicate that a huge energy barrier exists for a few

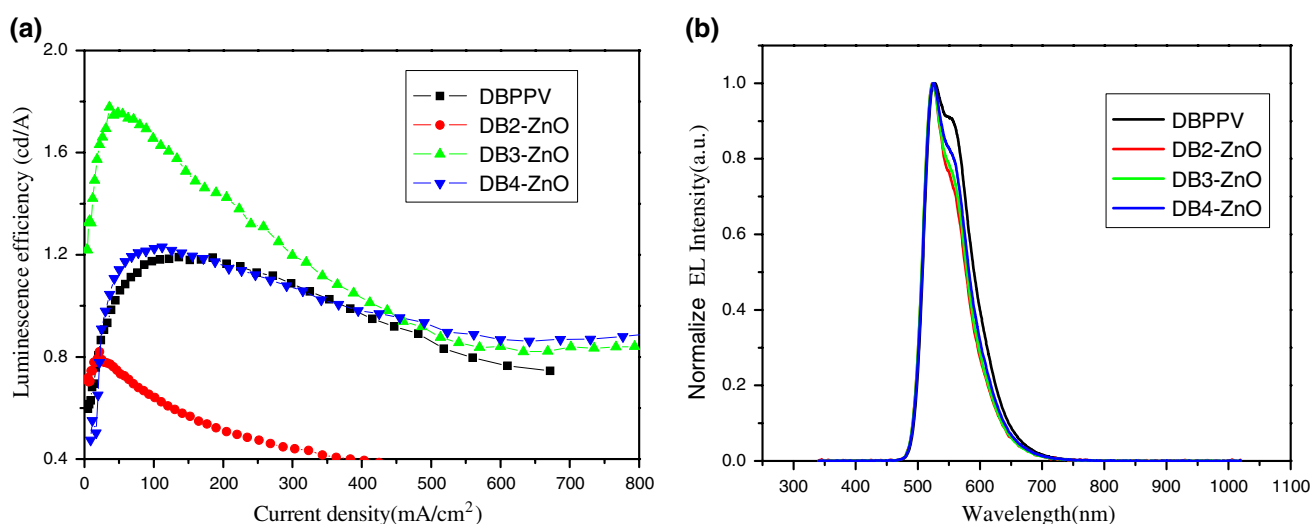


Fig. 2 **a** The luminescence efficiency versus current density curves and **b** normalized EL spectrum of characteristics of DBPPV, DB2–ZnO, DB3–ZnO and DB4–ZnO devices

Table 1 Performance of DBPPV–ZnO nano-composite based PLEDs

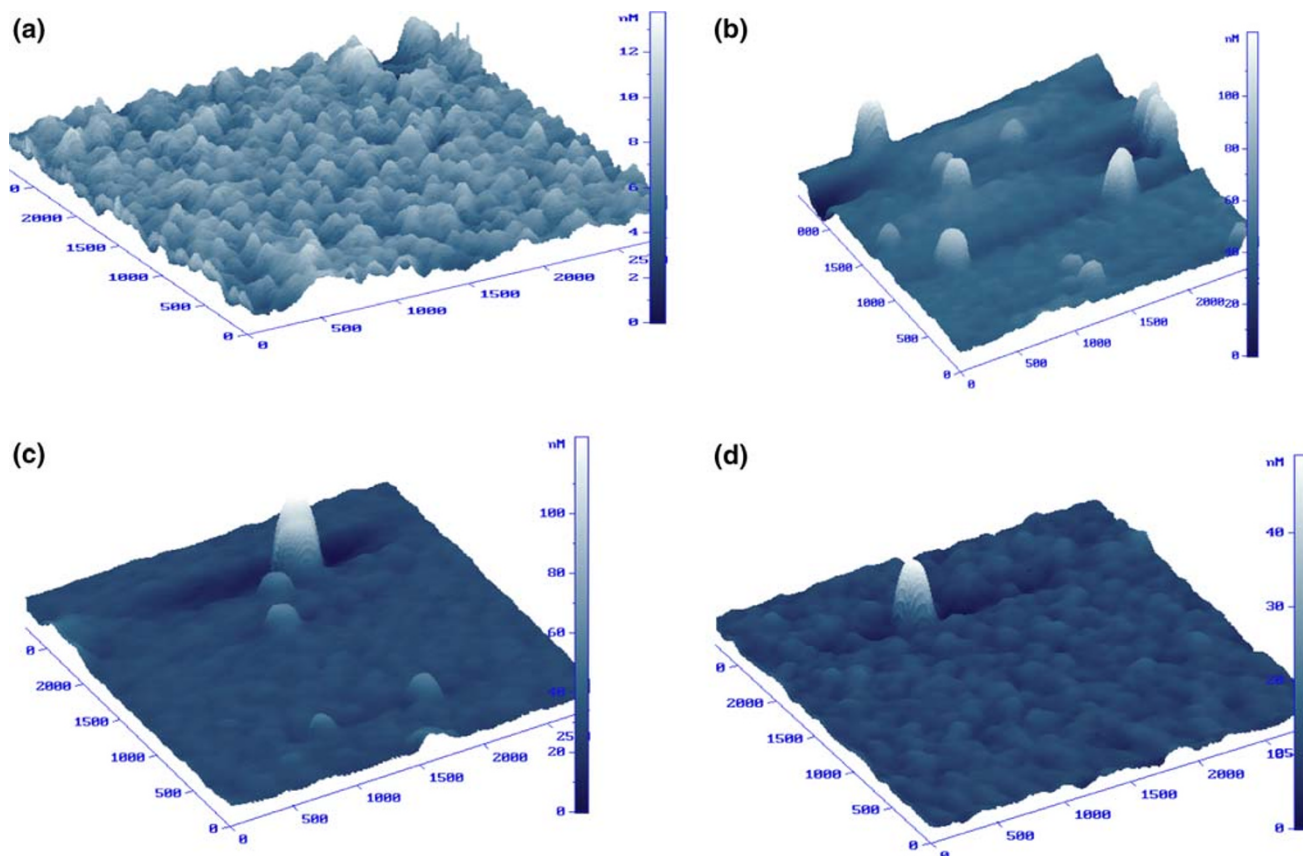
	DBPPV	DB3–ZnO	DB3–ZnO (annealing)
Turn-on (0.5 mA) (V)	3.76	3.10	3.38
Light turn-on (100 cd/m ²) (V)	4.10	3.225	3.25
Luminance efficiency (cd/A)	1.19	1.78	2.45

holes to be transferred from DBPPV to ZnO [20, 24]. When comparing the device performances, some important characteristics are observed. First of all, the luminance efficiency is significantly improved, for ZnO doping devices relative to that of pure DBPPV. The interface state between the metal oxide and polymer layers in the prepared device is critical determining factor for the optical performance and physical of polymer light emitting diodes. However, doping is still regarded as an effective technique to adjust the interfacial energy level distribution in processing electronic and optical devices.

The normalized EL as a function of the emission wavelength (nm) of PLEDs with pure DBPPV, DB2–ZnO, DB3–ZnO and DB4–ZnO are shown in Fig. 2b. We obviously found that for ZnO-doped DBPPV, the emission peak

from the inter-chain vibration of DBPPV was reduced, which perhaps is the possible reason that the nanoparticles assist the polymer arrangement and reduce the conformational disorder of polymer in the emission layer, and then cause the probability for inter-chain emission of device to reduce. It is observed that the emission peak only takes place in the emission layer and no emission from the inorganic layer is observed for the DB–ZnO devices. At the DBPPV–ZnO layer, the barrier potential of ZnO for holes is about 2.2 eV. The mobility of electrons in the ZnO is higher than that of holes in the DBPPV layer [25]. So the recombination zone of electrons and holes is primarily restricted to the DBPPV. This is the reason that the emission from DBPPV and the emission from the ZnO are not observed in the DB–ZnO devices.

Figure 3 shows the surface topography images of the four films coated on the same substrate ITO/PEDOT: (a) DBPPV layer, (b) DB2–ZnO, (c) DB3–ZnO and (d) DB4–ZnO materials. The roughness of the surface of the spin-coated sample film changed significantly. The increased roughness caused by the capillary attraction between the polymer and the ZnO nanoparticles increased the interfacial area between the sample film and the Ca/Al cathode and thus facilitated electron injection. The root-mean-

**Fig. 3** AFM 3D images of **a** DBPPV; **b** DB2–ZnO; **c** DB3–ZnO and **d** DB4–ZnO devices

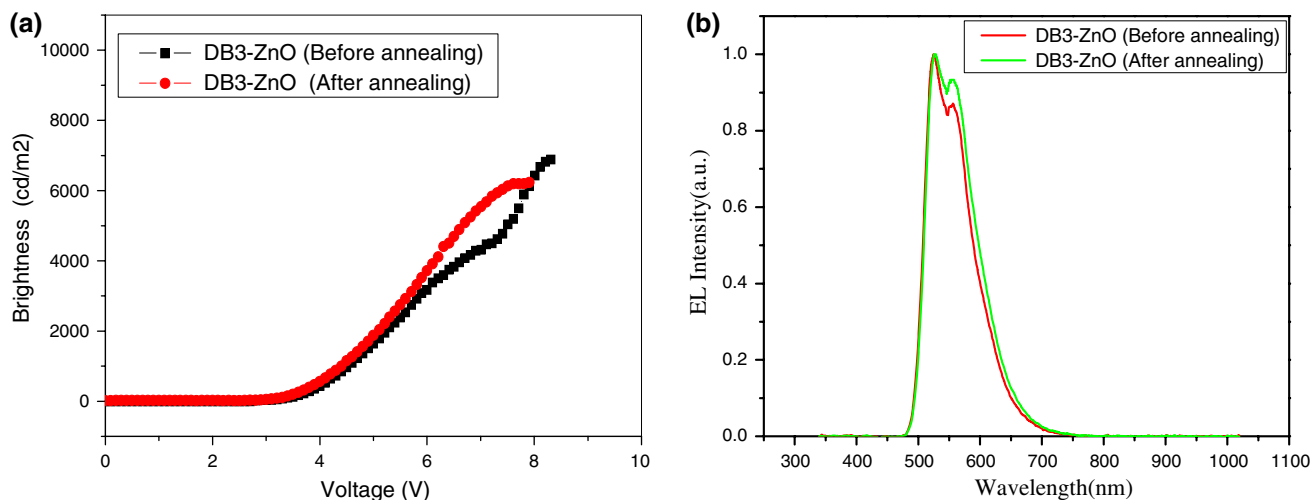


Fig. 4 **a** Brightness–voltage and **b** normalized EL spectrum characteristics of the DB3–ZnO annealed at 120 °C

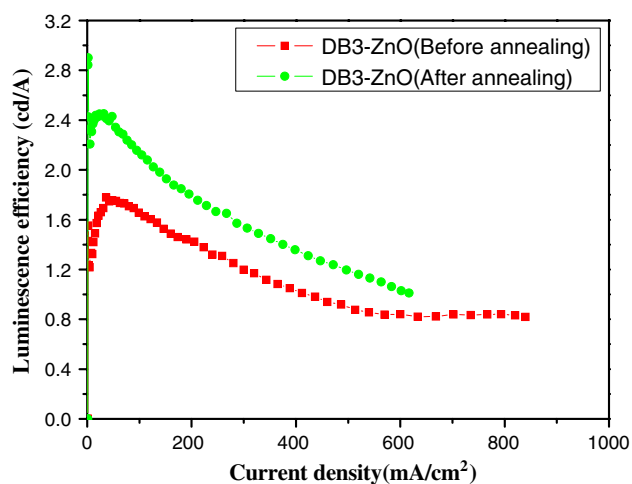


Fig. 5 The luminescence efficiency versus current density curves of DB3–ZnO devices before and after annealing

square (RMS) roughness of the films are DBPPV (1.5 nm), DB4–ZnO (3.02 nm), DB3–ZnO (8.778 nm) and DB2–ZnO (11.502 nm), respectively. A similar effect on surface roughness has been observed by other researchers in a Poly(9,9-dioctylfluorene-*alt*-thiophene copolymer (PDOFT)-gold nanoparticle(Au NPs) nanocomposite materials, and the performance of their device was improved by the addition of Au nanoparticles [26]. DB2–ZnO device is not significantly better than DBPPV, because of the increases in the rms roughness of DB2–ZnO materials could be attributed to the large amount of ZnO so that they could behave as matrix materials. DB2–ZnO nanocomposite induced the great variation of surface morphology and this was revealed to be the main reason of the conductivity change including the effect of local blocking of electron

conduction due to the agglomeration of the nanoparticles when introducing excess ZnO nanoparticle.

The mechanism for the current density and luminance enhancement in a PLED is not yet fully understood. Carter et al. demonstrated that the radiance increase is not due to microcavity effects resulting from the insulating oxide particles since no line-narrowing effects are observed [23]. Furthermore, the radiance enhancement is independent of the refractive index of the nanoparticles, scattering effects can also be excluded. Finally, an increase of the recombination at a polymer–nanoparticle interface would result in an increased efficiency, which is not observed and cannot explain the current enhancement. Carter and Blom et al. suggested that the current and radiance enhancement might arise from a change in the device morphology [13, 23]. A rougher cathode interface may give rise to an enhancement of the surface area with a resulting increase of electron injection. In addition, the existence of thin spots created throughout the film by capillary forces would give rise to an increase of the electric field, enhancing the charge injection and/or charge transport.

Figure 4a and b shows the brightness versus voltage and EL spectrum characteristics of a DB3–ZnO device after annealing at 120 °C for 30 min, respectively. Thermal annealing of the device slightly increased the brightness. The effect is attributed to the formation of an interfacial layer between the polymer and the metal electrodes [27]. The EL spectrum of a DB3–ZnO device before and after annealing consisted of a two EL peaks, one main peak (P1) and one shoulder peak (P2), in the spectra for the samples. The peak positions of the wavelength light emitted from the PLED before annealing are 525 nm (P1) and 560 (P2). Both peak positions of the wavelength of light emitted become slightly longer (redshift) when the PLED is annealed. Figure 5 shows that luminance efficiency versus

current density curves of a DB3–ZnO device before and after annealing. The carriers are transferred more effectively in PLEDs annealed at 120 °C because of the higher packing density of the DBPPV polymer film. It is a possible cause for the high luminescence and high efficiency of PLEDs annealed at 120 °C. In the case of the PLEDs fabricated with DB3–ZnO, the luminance efficiency increased by a factor of 30–40 after thermal annealing. Tu and Su [28] have suggested that the annealing temperature around the glass temperature of polymer materials can enhance the crystallization in the thin film and improve the morphology of the polymer film.

Conclusions

In summary, polymer light-emitting devices based on ZnO nanoparticle doped with DBPPV polymer matrix have been technically prepared by the solution-based spin coating technique. Current density–voltage and brightness–voltage characteristics demonstrated that the ZnO nanoparticle have the ability to improve the current density, brightness and luminance efficiency, which may be caused by the enhancement of charge injection and charge transport. From the EL spectrum, shoulder peak intensity of nanocomposite devices decreased suggesting that the nanoparticle reduced the conformational disorder of the polymer. The brightness and luminance efficiency of the PLEDs could be improved by annealing, for the DB3–ZnO device investigated. DB3–ZnO device shows maximum luminance efficiencies (1.78 cd/A) and with annealing (2.45 cd/A) having a brightness 643 and 776 cd/m² at a current density of 36.16 and 31.67 mA/cm², respectively. We have assumed that the annealing results in formation of a thin interfacial layer between the Ca cathode and nanocomposite film. Because of simple device structure and easily controllable fabricating conditions, this method has a high potential for the practical application of flat panel displays.

Acknowledgements The authors would like to thank Office of R&D, National Cheng Kung University, Taiwan, ROC.

References

1. J. Kalinowski, *Organic Light Emitting Diodes: Principles, Characteristics, and Processes* (Dekker, New York, 2005)
2. L. Bozano, S.A. Carter, J.C. Scott, G.G. Malliaras, P.J. Brock, *Appl. Phys. Lett.* **74**, 1132 (1999). doi:10.1063/1.123959
3. S.Y. Quan, F. Teng, Z. Xu, D.D. Wang, S.Y. Yang, Y.B. Hou, Y.S. Wang, *Phys. Lett. A* **352**, 434 (2006). doi:10.1016/j.physleta.2005.11.078
4. F.S. Li, Z.J. Chen, W. Wei, Q.H. Gong, *Org. Electron.* **6**, 237 (2005). doi:10.1016/j.orgel.2005.08.002
5. Y.M. Wang, F. Teng, Q.C. Zhou, Y.S. Wang, *Appl. Surf. Sci.* **252**, 2355 (2006). doi:10.1016/j.apsusc.2005.04.006
6. C. Tengstedt, A. Crispin, C.H. Hsu, C. Zhang, D. Parker, W.R. Salareck, M. Fahhman, *Org. Electron.* **6**, 21 (2005). doi:10.1016/j.orgel.2005.02.001
7. H.S. Yang, P.H. Holloway, *J. Phys. Chem. B* **107**, 9705 (2003). doi:10.1021/jp034749i
8. M.C. Suh, H.K. Chung, S.-Y. Kim, J.H. Kwon, B.D. Chin, *Chem. Phys. Lett.* **413**, 205 (2005). doi:10.1016/j.cplett.2005.07.082
9. M.Y. Chan, S.L. Lai, M.K. Fung, C.S. Lee, S.T. Lee, *Chem. Phys. Lett.* **374**, 215 (2003). doi:10.1016/S0009-2614(03)00675-4
10. C.S. Sulliyon, W.K. Woo, J.S. Steckel, M. Bawendi, V. Bulovic, *Org. Electron.* **4**, 123 (2003). doi:10.1016/j.orgel.2003.08.016
11. M. Cocchi, J. Kalinowski, D. Virgili, J.A.G. Williams, *Appl. Phys. Lett.* **92**, 113302 (2008). doi:10.1063/1.2898159
12. S. Welter, K. Brunner, J.W. Hofstraat, L. De Cola, *Nature* **421**, 54 (2003). doi:10.1038/nature01309
13. P.W.M. Blom, H.F. Schoo, M. Matters, *Appl. Phys. Lett.* **73**, 3914 (1998). doi:10.1063/1.122934
14. A.C. Arango, S.A. Carter, *Appl. Phys. Lett.* **74**, 1698 (1999). doi:10.1063/1.123659
15. C.Y. Kwong, W.C.H. Choy, A.B. Djuricic, P.C. Chui, K.W. Cheng, W.K. Chan, *Nanotechnology* **15**, 1156 (2004). doi:10.1088/0957-4484/15/9/008
16. A. Kiesow, S. Strohkark, K. Loschner, A. Heilmann, A. Podipensky, A. Abdolvand, G. Seifert, *Appl. Phys. Lett.* **86**, 153111 (2005). doi:10.1063/1.1897052
17. R. Shenhar, T.B. Norsten, V.M. Rotello, *Adv. Mater.* **17**, 657 (2005). doi:10.1002/adma.200401291
18. Z.W. Pan, Z.R. Dai, Z.L. Wang, *Science* **291**, 1947 (2001). doi:10.1126/science.1058120
19. P. Yang, H. Yan, S. Mao, R. Russo, J. Johnson, R. Saykally, N. Morries, J. Pham, R. He, H. Choi, *Adv. Funct. Mater.* **12**, 323 (2002). doi:10.1002/1616-3028(20020517)12:5<323::AID-ADFM323>3.0.CO;2-G
20. Z.X. Xu, V.A.L. Roy, P. Stallinga, M. Muccini, S. Toffanin, H.F. Xiang, C.M. Che, *Appl. Phys. Lett.* **90**, 223509 (2007). doi:10.1063/1.2740478
21. C. Fluerau, S. Schrader, V. Zauls, H. Motschmann, B. Stiller, R. Kiebooms, *Synth. Metal.* **111–112**, 603 (2000)
22. R.K. Ligan, L. Mangolini, U.R. Kortshagen, S.A. Campbell, *Appl. Phys. Lett.* **90**, 061116 (2007)
23. S.A. Carter, J.C. Scott, P.J. Brock, *Appl. Phys. Lett.* **71**, 1145 (1997)
24. D.H. Hu, Z.B. Deng, Y. Xu, J. Xiao, C.J. Liang, H.Y. Zhao, Z.P. Liu, *Mater. Sci. Eng. B* **122**, 179 (2005)
25. J. Huang, Z. Xu, S. Zhao, Y. Li, F. Zhang, L. Song, Y. Wang, X. Xu, *Solid State Commun.* **142**, 417 (2007)
26. S.H. Wu, H.M. Huang, K.C. Chen, C.W. Hu, C.C. Hsu, C.C. Tsiang, *Adv. Funct. Mater.* **16**, 1959 (2006)
27. J.H. Ahn, C. Wang, N.E. Widdowson, C. Pearson, M.R. Bryce, M.C. Petty, *J. Appl. Phys.* **98**, 054508 (2005)
28. M.L. Tu, Y.K. Su, W.C. Lu, *Jpn J. Appl. Phys.* **45**(10A), 7737 (2006)